Title: Modified Gravity (MOG) and Dark Matter: Can We Detect Dark Matter in the Present Universe?

Date: Nov 20, 2014 11:00 AM

URL: http://pirsa.org/14110133

Abstract: A modified gravity (MOG) theory is explored that can explain current observational data in the present universe without detectable dark matter. This data includes galaxy rotation curves, cluster dynamics, gravitational lensing, globular clusters, the Bullet Cluster and solar system experiments. A vector field in the MOG action is a hidden, dark and massive photon that acts as a collisionless particle in the early universe and explains structure growth. The vector field evolves to an ultralight hidden photon in the present universe after the formation of stars and galaxies, and it cannot play the role of detectable dark matter. The theory successfully describes the CMB data. The matter power spectrum is fitted without dark matter and can distinguish between modified gravity and dark matter scenarios in the present universe.

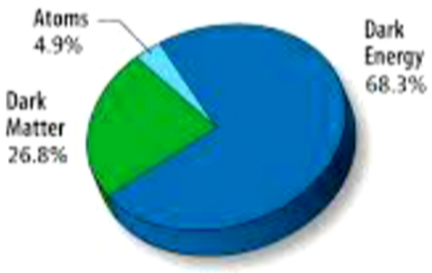

TODAY

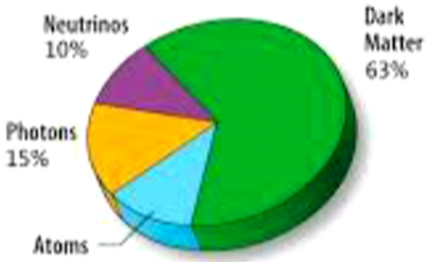

13.7 BILLION YEARS AGO
(Universe 380,000 years old)

1. Introduction

Observations of the dynamics of galaxies as well as the dynamics of the whole Universe reveal that a main part of the Universe's mass must be missing or, in modern terminology, this missing mass is made of dark matter. The universe is observed to undergo an accelerated expansion (dark energy).

Observations of galaxies reveal that there is a discrepancy between the observed dynamics and the mass inferred from luminous matter (Rubin et al. 1965, Rubin & Ford 1970).

An alternative approach to the problem of missing mass is to replace dark matter by a modified gravity theory. The generally covariant Modified Gravity (MOG) theory is a scalar-tensor-vector theory (STVG, JM, JCAP, 0603 004 (2006), arXiv:0506021 [gr-qc]).

The LUX experimental data from the Sanford Underground Research Facility (Lead, South Dakota) using a 370 kg liquid Xenon detector has ruled out low-mass WIMPs, and set new bounds on elastic scattering cross sections of WIMPs. No WIMP signals were detected. To-date no convincing detection of dark matter particles has been achieved in either laboratory or satellite experiments.

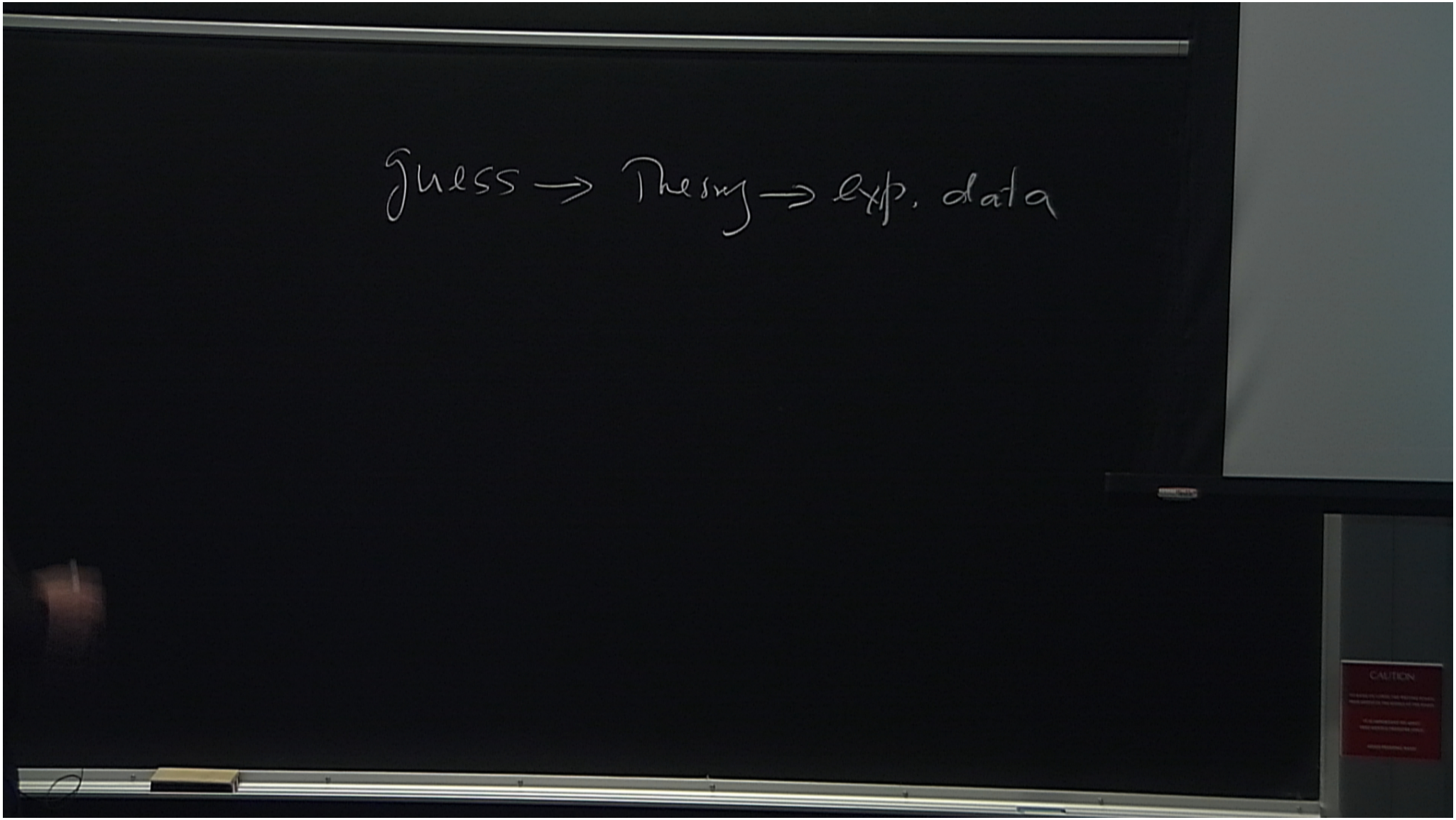
Guess → Theory → Exp. data
CAUTION

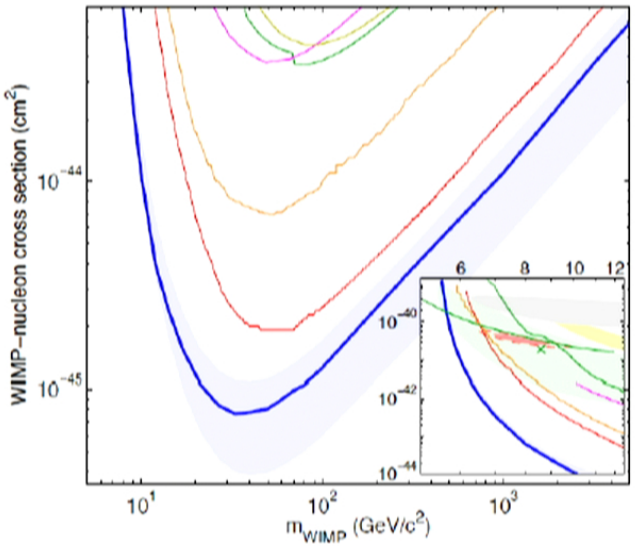

FIG. 5. The LUX 90% confidence limit on the spin-independent elastic WIMP-nucleon cross section (blue), together with the $\pm 1\sigma$ variation from repeated trials, where trials fluctuating below the expected number of events for zero BG are forced to 2.3 (blue shaded). We also show Edelweiss II [41] (dark yellow line), CDMS II [42] (green line), ZEPLIN-III [43] (magenta line) and XENON100 100 live-day [44] (orange line), and 225 live-day [45] (red line) results. The inset (same axis units) also shows the regions measured from annual modulation in CoGeNT [46] (light red, shaded), along with exclusion limits from low threshold re-analysis of CDMS II data [47] (upper green line), 95% allowed region from CDMS II silicon detectors [48] (green shaded) and centroid (green x), 90% allowed region from CRESST II [49] (yellow shaded) and DAMA/LIBRA allowed region [50] interpreted by [51] (grey shaded).

Experimental data that must be explained and fitted by MOG:

1. Planck and WMAP cosmic microwave background (CMB) data:
   Structure growth (stars and galaxies)
   Angular acoustical power spectrum
   Matter power spectrum
   Accelerated expansion of the universe.

2. Galaxy rotation curves and galaxy evolution and stability.

3. Galactic cluster dynamics.

4. Bullet Cluster 1E0657-558 and Abell 520 cluster "train wreck" collision.

5. Gravitational lensing in cosmology.

6. Binary pulsar timing (PSR 1913+16).

7. Solar system experiments:
   Weak equivalence experiments, light deflection by Sun, Shapiro time delay (Cassini probe), planetary orbits.

2. MOG FIELD EQUATIONS

The MOG action is given by (STVG, JM 2006):

$$S = S_G + S_\phi + S_S + S_{\rm EM} + S_M$$

where

$$S_G = \frac{1}{16\pi}\int d^4x\sqrt{-g}\Big[\frac{1}{G}(R+2\Lambda)\Big]$$

$$S_\phi = -\omega\int d^4x\sqrt{-g}\Big[\frac{1}{4}B^{\mu\nu}B_{\mu\nu} - V(\phi)\Big] \quad B_{\mu\nu} = \partial_\mu\phi_\nu - \partial_\nu\phi_\mu \qquad (\omega = 1)$$

$$S_S = \int d^4x\sqrt{-g}\Big[\frac{1}{G^3}\Big(\frac{1}{2}g^{\mu\nu}\nabla_\mu G\nabla_\nu G - V(G)\Big) + \frac{1}{\mu^2 G}\Big(\frac{1}{2}g^{\mu\nu}\nabla_\mu\mu\nabla_\nu\mu - V(\mu)\Big)\Big]$$

$$S_{\rm EM} = -\frac{1}{4}\int d^4x\sqrt{-g}F^{\mu\nu}F_{\mu\nu}$$

$$G_{\mu\nu} - g_{\mu\nu}\Lambda + Q_{\mu\nu} = 8\pi G T_{\mu\nu} \qquad Q_{\mu\nu} = G\Big(g^{\alpha\beta}\Theta\nabla_\alpha\nabla_\beta g_{\mu\nu} - \nabla_\mu\nabla_\nu\Theta\Big)$$

$$\Theta(x) = G^{-1}(x)$$

The action for pressureless dust can be written as

$$S_M = \int \left(-\rho\sqrt{u^\mu u_\mu} - \omega Q_5 u^\mu \phi_\mu\right)\sqrt{-g}\,\mathrm{d}x^4.$$

Here, ρ is the density of matter and Q_5 is the fifth force source charge, which is related to the mass density, $Q_5 = \kappa\rho$, where κ is a constant.

$$\kappa = \pm\sqrt{\frac{\alpha G}{4\pi}} \qquad Q = \pm\sqrt{\frac{\alpha G}{4\pi}}M \qquad (\omega = 1)$$

We choose the positive root for the gravitational charge, Q > 0.

Varying the action with respect to the fields results in the MOG field equations. The variation of the actions S_M , S_ϕ and S_S and S_{EM} with respect to the metric yields the energy-momentum tensor:

$$T_{\mu\nu} = T_{M\mu\nu} + T_{\phi\mu\nu} + T_{S\mu\nu} + T_{EM}$$

$$T_{X\mu\nu} = -\frac{2}{\sqrt{-g}}\frac{\delta S_X}{\delta g^{\mu\nu}}, \quad (X = [M, \phi, S, EM]).$$

A test particle obeys the modified weak field Newtonian acceleration law:

$$\ddot{r} = -\frac{G_N M}{r^2}\left[1 + \alpha - \alpha(1+\mu r)e^{-\mu r}\right]$$

$$\Phi(r) = -\frac{G_N M}{r}\left[1 + \alpha - \alpha e^{-\mu r}\right]$$

For an extended distribution of matter:

$$\nabla^2\Phi(\mathbf{r}) = 4\pi G_N \rho(\mathbf{r}) + \alpha\mu^2 G_N \int \frac{e^{-\mu|\mathbf{r}-\tilde{\mathbf{r}}|}}{|\mathbf{r}-\tilde{\mathbf{r}}|}\rho(\tilde{\mathbf{r}})\; d^3\tilde{\mathbf{r}}$$

A photon follows a null-geodesic path:

$$\frac{dk^\mu}{d\lambda} + \Gamma^\nu{}_{\alpha\beta}k^\alpha k^\beta = 0$$

k^μ = photon momentum

We invoke a screening mechanism in dense environments due to the non-linearity of the interaction potentials and their coupling strengths . This will be important for photon paths.

The action for the scalar field G can be written as (1/G = χ^2 /2):

$$S_\chi = \int d^4x\sqrt{-g}\left(\frac{1}{2}g^{\mu\nu}\nabla_\mu\chi\nabla_\nu\chi - V(\chi)\right)$$

The conformal metric in the Jordan frame is connected to $g_{\mu\nu}$ by the conformal transformation:

$$\tilde{g}_{\mu\nu} = A^2(\chi)g_{\mu\nu}, \quad \tilde{g} = \mathrm{Det}\tilde{g}_{\mu\nu} = A^8(\chi)g$$

$$\nabla_\mu T^{\mu\nu} = \frac{d\ln A(\chi)}{d\chi}(g^{\mu\nu}T - T^{\mu\nu})\nabla_\mu\chi,$$

$$V_{\mathrm{eff}}(\chi) = V(\chi) - (A(\chi) - 1)T_M \quad V(\chi) = -\frac{1}{2}\mu_\chi^2\chi^2 + W(\chi)$$

$$m_\chi^2 = \frac{d^2V_{\mathrm{eff}}(\chi)}{d\chi^2}\Big|_{\chi=\chi_{\mathrm{min}}} > 0$$

The ultra-relativistic massless photon coupled to matter is screened by the effective gravitational constant $\tilde{G}$ due to the mass $m_\chi(\rho)$ screening mechanism.

$$\tilde{G} = C(\chi(\rho))G. \qquad \tilde{G} = C(\alpha(\rho))G_N(1+\alpha) \qquad \alpha = \frac{(G_\infty - G_N)}{G_N}$$

For a point mass M the potential experienced by a photon is

$$\Phi_{\rm eff} = \frac{\tilde{G}(\chi(\rho))M}{r} = \frac{G_N M}{r}[1 + 2h^2(\chi)\exp(-\mu_\chi r)]$$

For an extended distribution of matter we have

$$\Phi_{\rm eff} = G_N \int d^3x' \frac{\rho(\mathbf{x}')}{|\mathbf{x}-\mathbf{x}'|}[1 + 2h^2(\chi)\exp(-\mu_\chi|\mathbf{x}-\mathbf{x}'|)]$$

We have two screening mechanisms in MOG. One is due to the repulsive gravitational Yukawa force, and the other is due to the attractive scalar field χ. The vector field ϕ_μ and the scalar field χ screen the local gravitational field in the vicinity of the Sun and earth, guaranteeing agreement of MOG with solar system experiments. They also screen the gravitational radiation emitted indirectly by binary pulsars (pulsar timing), so that only quadrupole radiation is detected in the wave zone. (JWM, arXiv:1410.2464 [gr-qc]. See also: JWM and V. T. Toth, MNRAS, 397, 1885 (2009), arXiv: 0805.4774 [astro-ph]).

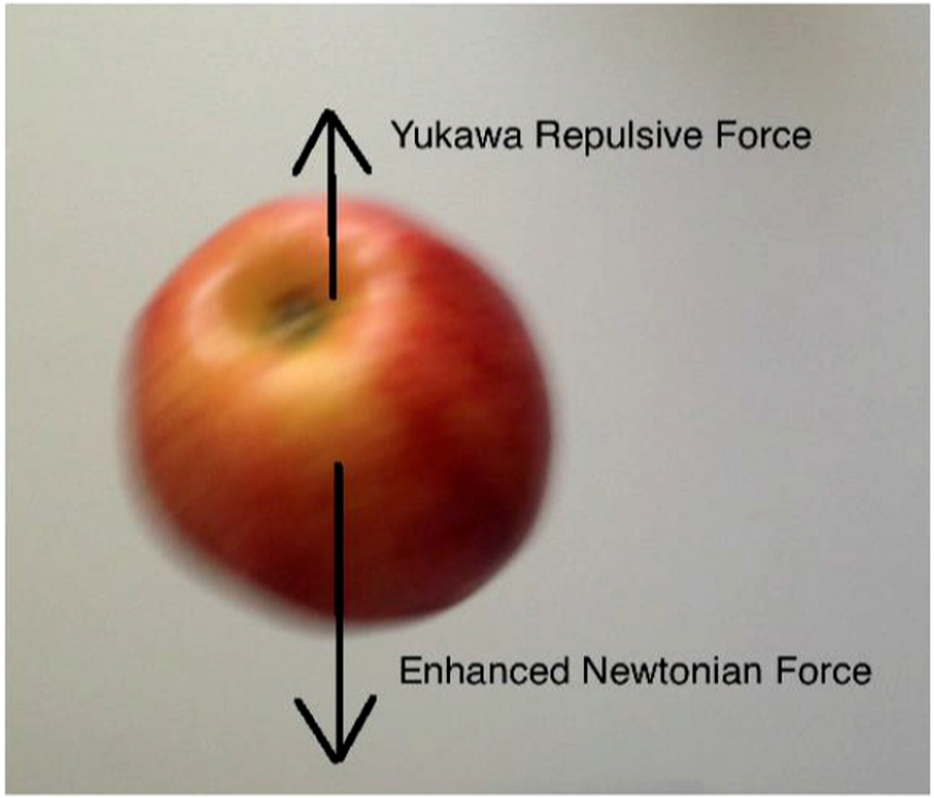

Credit: Picture is taken by Sepehr Rahvar

Big bang at t = 0 followed by either inflationary expansion period or by variable speed of light (VSL) with $c > c_0$ (c_0 = measured speed of light today).

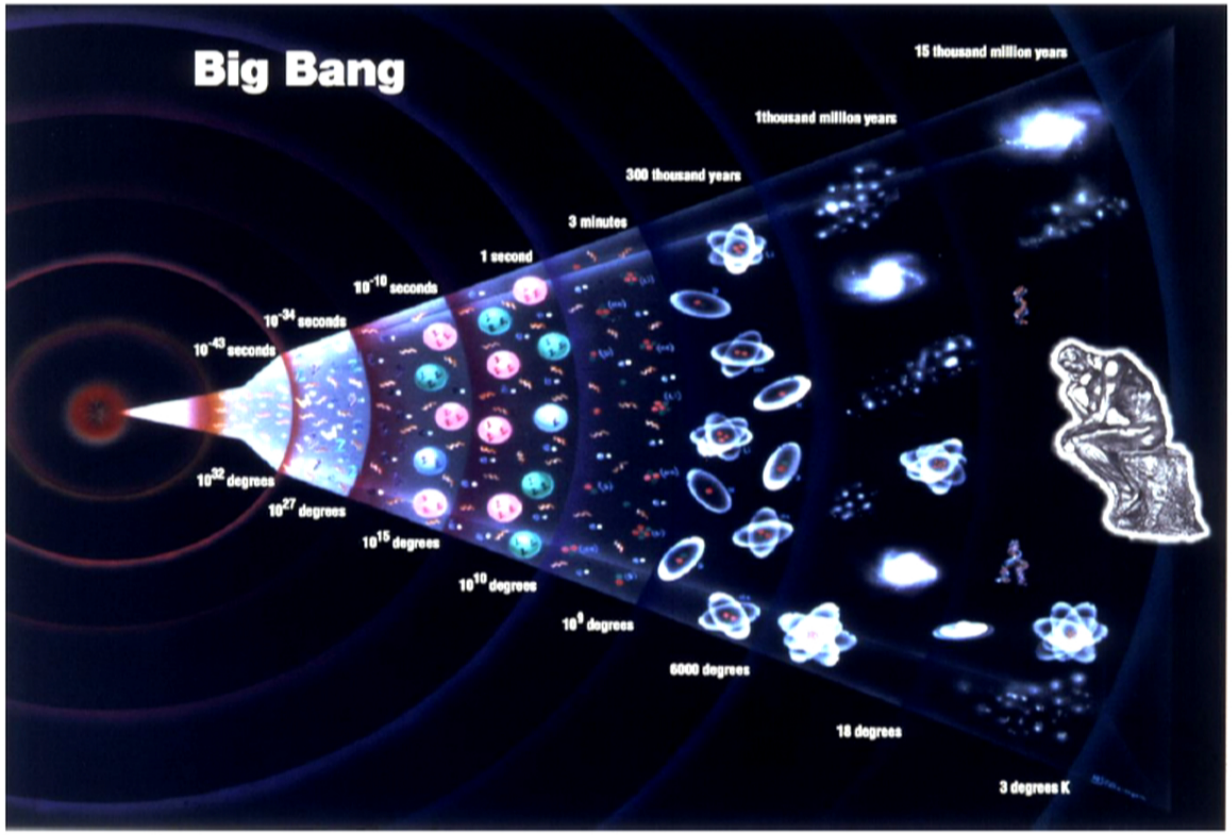

3. MOG Cosmology (JWM, arXiv:1409.0853 [astro-ph.CO]).

We base our cosmology on the homogeneous and isotropic Friedmann-Lemaitre-Robertson-Walker (FLRW) background metric:

$$ds^2 = dt^2 - a^2(t)\left(\frac{dr^2}{1-Kr^2} + r^2(d\theta^2 + \sin^2\theta d\phi^2)\right)$$

We use the energy-momentun tensor of a perfect fluid:

$$T_{\mu\nu} = (\rho + p)u_\mu u_\nu - p g_{\mu\nu} \qquad \rho = \rho_M + \rho_\phi + \rho_G + \rho_\mu$$

The MOG Friedmann equations are given by:

$$\left(\frac{\dot{a}}{a}\right)^2 + \frac{K}{a^2} = \frac{8\pi G\rho}{3} + \frac{\dot{a}}{a}\frac{\dot{G}}{G} + \frac{\Lambda}{3},$$

$$\frac{\ddot{a}}{a} = -\frac{4\pi G}{3}(\rho + 3p) + \frac{1}{2}\left(\frac{\ddot{G}}{G} - \frac{2\dot{G}^2}{G^2} + \frac{\dot{a}\dot{G}}{aG}\right) + \frac{\Lambda}{3}$$

In the following, we assume a spatially flat universe $K = 0$. $\dot{G} \sim 0$, and we also assume that $\dot{\mu} \sim 0$.

$$H^2 = \frac{8\pi G\rho}{3} + \frac{\Lambda}{3},$$

$$\frac{\ddot{a}}{a} = -\frac{4\pi G}{3}(\rho + 3p) + \frac{\Lambda}{3} \qquad \dot{\rho} + 3\frac{d\ln a}{dt}(\rho + p) = 0$$

$$\delta\rho(\mathbf{r},\mathbf{t}) = \frac{1}{(2\pi)^{3/2}}\bar{\rho}\int d^3k\delta_{\mathbf{k}}(t)\exp(i(a_0/a)\mathbf{k}\cdot\mathbf{r})$$

$$\delta p(\mathbf{r},\mathbf{t}) = \frac{1}{(2\pi)^{3/2}}\int d^3k\delta p_{\mathbf{k}}(t)\exp(i(a_0/a)\mathbf{k}\cdot\mathbf{r}) \qquad k^2\Phi_{\mathbf{k}} = -4\pi G\left(\frac{a}{a_0}\right)^2\bar{\rho}\delta_{\mathbf{k}}.$$

$$\Phi(\mathbf{r},\mathbf{t}) = \frac{1}{(2\pi)^{3/2}}\int d^3k\Phi_{\mathbf{k}}(t)\exp(i(a_0/a)\mathbf{k}\cdot\mathbf{r}),$$

where $\delta = \delta\rho/\bar{\rho}$ is the relative density perturbation contrast.

The modified Newtonian acceleration law in MOG for a point particle is given by

$$\ddot{r} = -\frac{G_\infty M}{r^2}\left[1 - \frac{\alpha}{1+\alpha}(1+\mu r)\exp(-\mu r)\right],$$

$$\alpha = (G_\infty - G_N)/G_N \qquad G_\infty = G_N(1+\alpha)$$

The MOG potential for a given density $\rho(\mathbf{x})$ is

$$\Phi(\mathbf{x}) = -G_N \int d^3x' \frac{\rho(\mathbf{x}')}{|\mathbf{x}-\mathbf{x}'|}\left[1+\alpha-\alpha e^{-\mu|\mathbf{x}-\mathbf{x}'|}\right]$$

$$\frac{\partial \rho}{\partial t} + \nabla\cdot(\rho\mathbf{v}) = 0$$

$$\frac{\partial \mathbf{v}}{\partial t} + (\mathbf{v}\cdot\nabla)\mathbf{v} = -\frac{\nabla p}{p} - \nabla\Phi$$

The MOG Boltzmann equation is

$$\frac{\partial f}{\partial t} + \mathbf{v}\cdot\nabla f - \nabla\Phi\cdot\frac{\partial f}{\partial \mathbf{v}} = 0$$

$$\Omega_b = \frac{8\pi G_N \rho_b}{3H^2}, \quad \Omega_\phi = \frac{8\pi G_N \rho_\phi}{3H^2}, \quad \Omega_\Lambda = \frac{\Lambda}{3H^2}$$

In the present scenario there are five components to the energy density:

1. neutral pressureless phion particles (ϕ_μ field),
2. baryonic matter,
3. photons,
4. neutrinos,
5. Dark energy

Thus, we have

$$\rho = \rho_m + \rho_r + \rho_d,$$

where

$$\rho_m = \rho_b + \rho_\phi + \rho_G + \rho_\mu, \quad \rho_r = \rho_\gamma + \rho_\nu$$

and where $\rho_r, \rho_d, \rho_\gamma$ and ρ_ν denote the radiation, dark energy, photon and neutrino densities, respectively.

We assume that when ρ_ϕ dominates in the early universe before decoupling $\alpha < 1$.

$$G \sim G_\infty \sim G_N$$

At the time of big-bang-nucleosynthesis (BBN), we have $G \sim G_N$, guaranteeing that the production of elements agrees with observation. After decoupling $\rho_\phi \sim \rho_b$ until stellar and galaxy formation when $\rho_\phi \ll \rho_b$ and the MOG non-relativistic acceleration law sets in to explain the rotation curves of galaxies and the dynamics of clusters without detectable dark matter.

We assume that at horizon entry until some time after decoupling:

$$\rho_\phi \gg \rho_b,\ \rho_\phi \gg \rho_G,\ \rho_\phi \gg \rho_\mu$$

and $V_G = V_\mu = 0$. The first Friedman equation becomes

$$H^2 = \frac{8\pi G_N \rho_\phi}{3} + \frac{\Lambda}{3} \qquad \rho_\phi = \frac{1}{2}\omega\mu^2\phi_0^2 \qquad (\omega = 1)$$

The Jeans equation for density perturbations is

$$\ddot{\delta}_{\mathbf{k}} + 2H\dot{\delta}_{\mathbf{k}} + \left(\frac{c_s^2 a_0^2 k^2}{a^2} - 4\pi G_N \bar{\rho}\right)\delta_{\mathbf{k}} = 0 \qquad c_s = \sqrt{\frac{dp}{d\rho}}$$

The Proca vector field ϕ_μ is a neutral massive spin 1 particle (massive hidden photon). Because it does not couple to massless photons, it can be treated as almost pressureless. The pressure gradient term in the Jeans equation is absent and the speed of sound is zero, $c_s \sim 0$. We get

$$\ddot{\delta}_{\mathbf{k}} + 2H\dot{\delta}_{\mathbf{k}} - 4\pi G_N \bar{\rho}\delta_{\mathbf{k}} = 0$$

There is no oscillatory behavior of the phion particles and perturbations grow at all wave lengths. On the other hand, the baryon perturbations oscillate before decoupling, due to the photon-baryon pressure, producing baryon acoustical oscillations.

After decoupling the baryon density perturbations grow and catch up with the phion $\delta\rho_b$ density perturbations. The phion density perturbations solve the problem of getting sufficient growth to form stars and galaxies later in the universe.

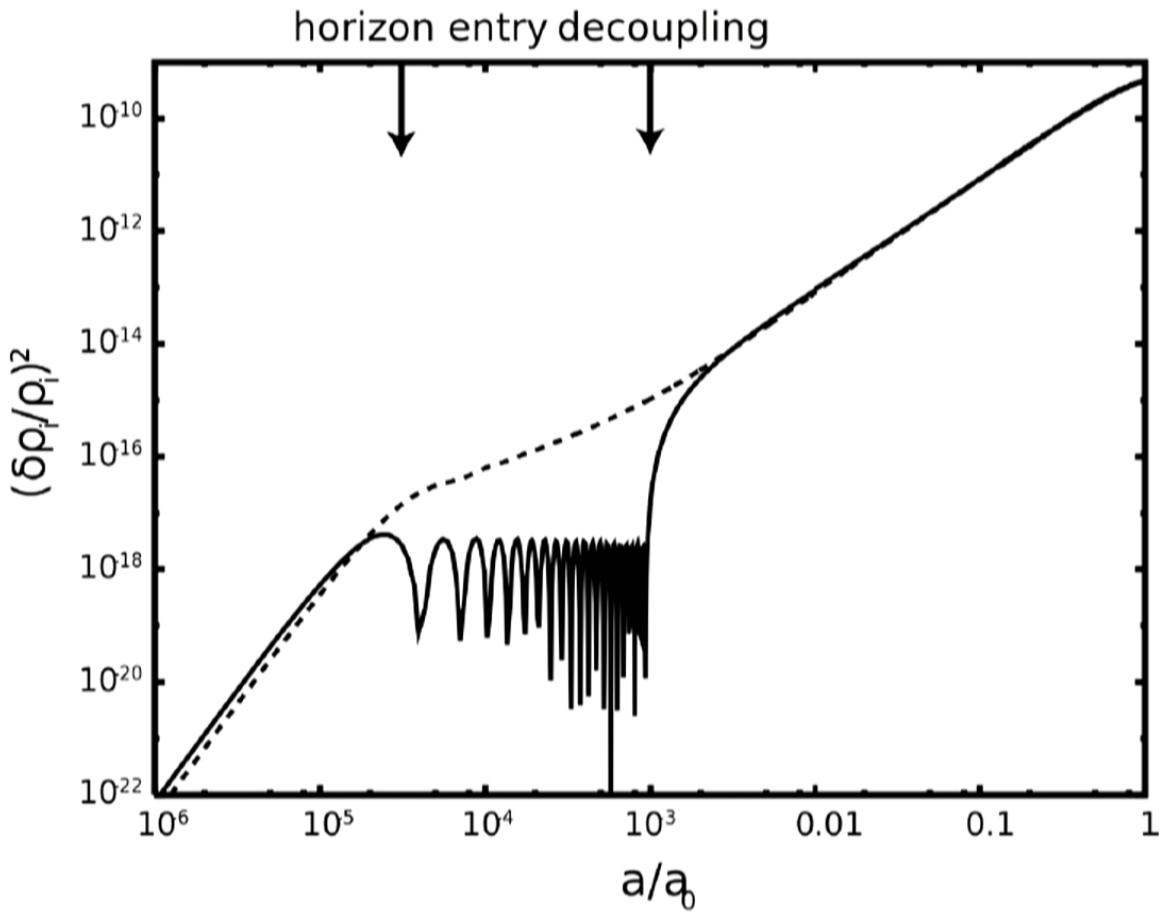
horizon entry decoupling
10^{10}
10^{12}
10^{14}
10^{16}
10^{18}
10^{20}
10^{22}
$(\delta\rho_r/\rho_i)^2$
10^6
10^5
10^4
10^3
0.01
0.1
1
a/a_0

As the universe expands beyond the time of decoupling, the gravitational attraction between baryons increases and $G = G_\infty = G_N(1+\alpha)$. Eventually, as the large scale structures form $\rho_\phi < \rho_b$ and the baryon dominated MOG takes over. The galaxy rotation curves and the galactic cluster dynamics are determined without dark matter. The best fit values for α and μ are:

$$\alpha = 8.89 \pm 0.34 \qquad \mu = 0.04 \pm 0.004\,\mathrm{kpc}^{-1}$$

The phion mass parameter is a scalar field which evolves with time as the universe expands. After horizon entry $m_\phi \gg 10^{-28}\,\mathrm{eV}$ and the phion particle behaves like cold dark matter (CDM). When the earliest stars and galaxies form, the phion mass undergoes a significant decrease. In the present universe from the best fit value $\mu = 0.04\,\mathrm{kpc}^{-1}$ we get $m_\phi = 2.6 \times 10^{-28}\,\mathrm{eV}$. The phion (hidden photon) mass becomes ultra-light and cannot contribute to the dynamics of galaxies and galactic clusters.

We conclude that dark matter particles cannot be detected in the present universe, either by laboratory experiments or in astrophysical observations (Pamela, AMS, gamma ray bursts).

The acoustical angular power spectrum at the CMB can be calculated in MOG.

$$\Delta^2 = Ak^3T^2(k)P_0(k). \qquad T(k) = T_b(k) + T_\phi(k).$$

For a constant non-zero value of α, we have in the present universe $\rho_\phi \ll \rho_b$:

$$(G_N\rho)_{\Lambda CDM} = (G_N(1+\alpha)\rho)_{\rm MOG}. \quad \rho_{\Lambda CDM} = \rho_b + \rho_{CDM} \qquad \rho_{\rm MOG} = \rho_b$$

Now, red-shifting towards the CMB, ρ_ϕ becomes smoothly bigger than ρ_b and $\alpha << 1$:

$$(G_N\rho)_{\Lambda\rm CDM} = (G_N\rho_\phi)_{\rm MOG}$$

It follows that the angular acoustical power spectrum calculation can be duplicated in MOG using the Planck 2013 best-fit values:

$$\Omega_b h^2 = 0.022199. \quad \Omega_c h^2 = 0.11847,\ n_s = 0.9624,\ H_0 = 67.94\,{\rm km\,sec^{-1}\,Mpc^{-1}}$$

$\Omega_\Lambda = 0.6939$, $\sigma_8 = 0.8271$

The value of α today is $\alpha = 4.3367$.

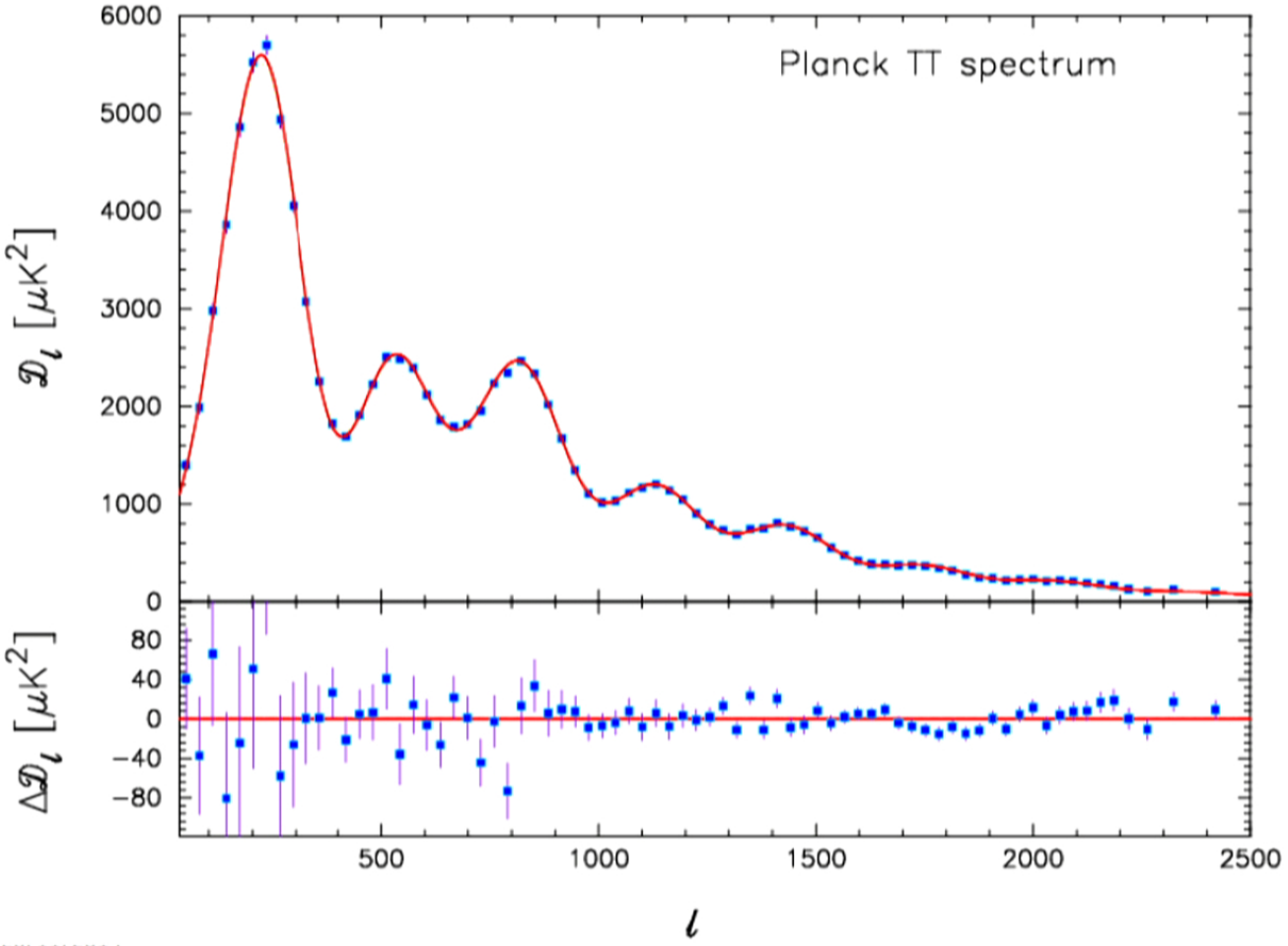
Planck TT spectrum
$\mathcal{D}_\ell$ [μK^2]
$\Delta\mathcal{D}_\ell$ [μK^2]
ℓ
6000
5000
4000
3000
2000
1000
0
80
40
0
−40
−80
500
1000
1500
2000
2500

The matter power spectrum determined by the distribution of matter obtained from large scale galaxy surveys can also be predicted by MOG. A suitable window function and an initial scale invariant power spectrum P_0 are chosen to determine P(k). Baryon unit oscillations are greatly dampened by the window function.

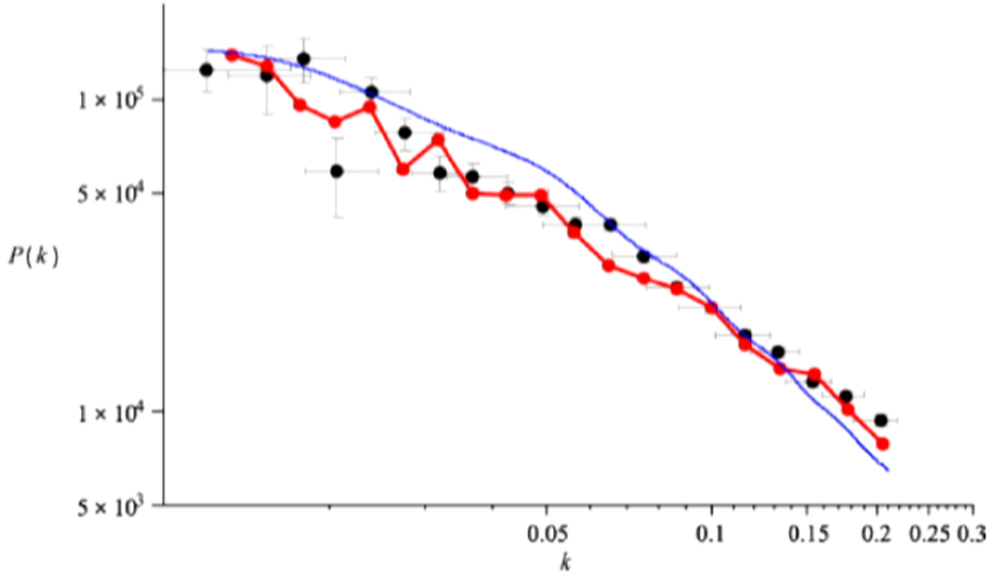

With a sufficiently large survey of galaxies, the unit baryon oscillations will begin to be observed and distinguish between MOG, without detectable dark matter, and the standard ΛCDM model without unit baryon oscillations. This is a generic test that can distinguish MOG from dark matter models.

Figure 1. The matter power spectrum. Three models are compared against five data sets (see text): Λ-cold dark matter (Λ-CDM) (dashed blue line, $\Omega_b = 0.035$, $\Omega_c = 0.245$,$\Omega_\Lambda = 0.72$, $H = 71$ km/s/Mpc), a baryon-only model (dotted green line, $\Omega_b = 0.035$, $H = 71$ km/s/Mpc) and modified gravity (MOG) (solid red line, $\alpha = 19$, $\mu = 5$ h Mpc^{-1}, $\Omega_b = 0.035$, $H = 71$ km/s/Mpc), Data points are colored light blue [Sloan Digital Sky Survey (SDSS) 2006], gold (SDSS 2004), pink [Two-degree-Field (2dF)], light green [UK Schmidt Telescope (UKST)] and dark blue (CfA).

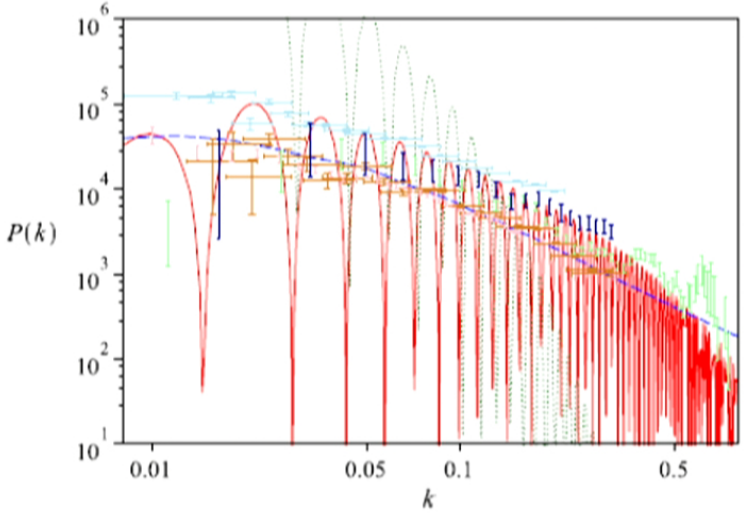

A prediction for the matter power spectrum that can distinguish MOG, without dark matter, from the standard ΛCDM model. Data from Battye, Charnock and Moss (arXiv:1409.269, to appear in MNRAS).

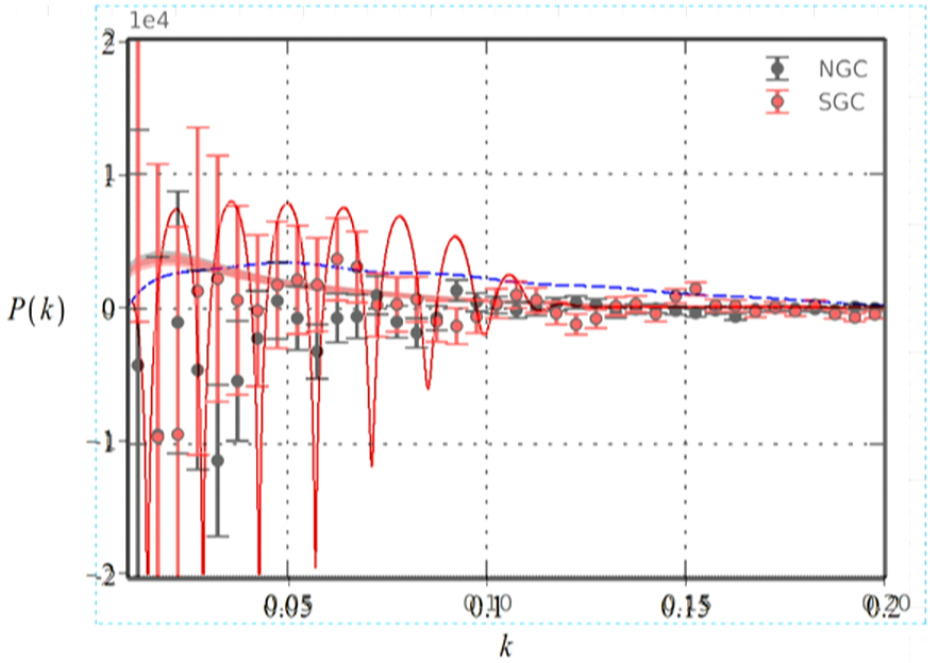

Accelerated expansion of the universe. Dark energy can be explained by the cosmological constant Λ or by the MOG potential V(G).

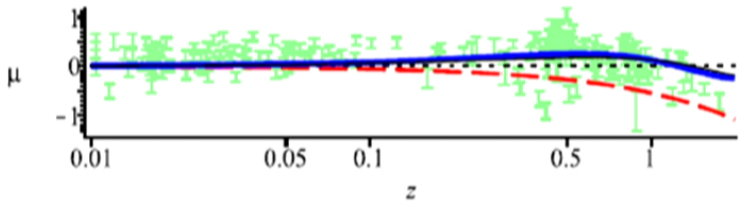

FIGURE 8. Type Ia supernova luminosity-redshift data [22] and the MOG/ΛCDM predictions. The horizontal axis corresponds to the $q = 0$ empty universe. The MOG result is represented by a thick (blue) line. Dashed (red) line is a matter-dominated Einstein de-Sitter universe with $\Omega_M = 1$, $q = 0.5$. Thin (black) line is the ΛCDM prediction.

4. ROTATION CURVES OF GALAXIES (JWM & S. Rahvar, MNRAS 436, 1439 (2013), arXiv: 1306.6383 [astro-ph]).

Recent applications of MOG to galaxy dynamics is based on continuous distributions of baryon matter and realistic models of galaxy bulges and disks.

We choose a subsample of nearby galaxies from the THINGS catalogue with high-resolution measurements of velocity and density of hydrogen profile (de Blok et al. 2008). For this set of galaxies, we adopt in the weak field approximation μ and α as well as the stellar mass-to-light ratio M/L when fitting the rotation curves of galaxies to the data. We then find the best values of α and μ and fix these two parameters. Then, we fit the observed rotation curves of the larger Ursa Major sample of galaxies, letting the stellar mass-to-light ratio M/L be the only free parameter.

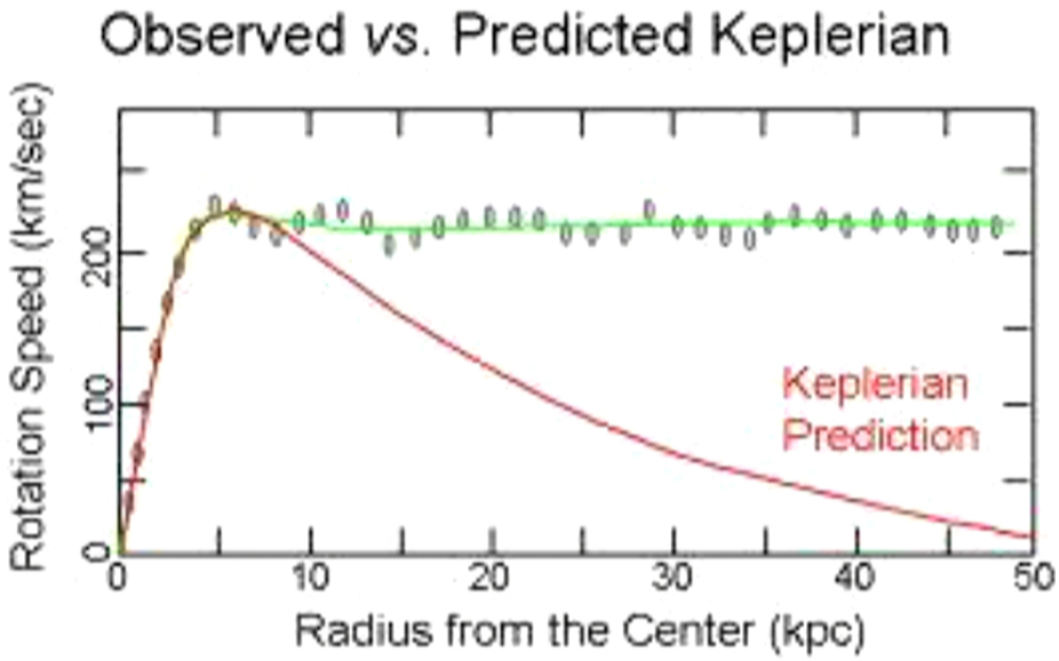
Observed vs. Predicted Keplerian
Rotation Speed (km/sec)
0
100
200
0
10
20
30
40
50
Radius from the Center (kpc)
Keplerian
Prediction

THINGS – The HI nearby galaxy survey

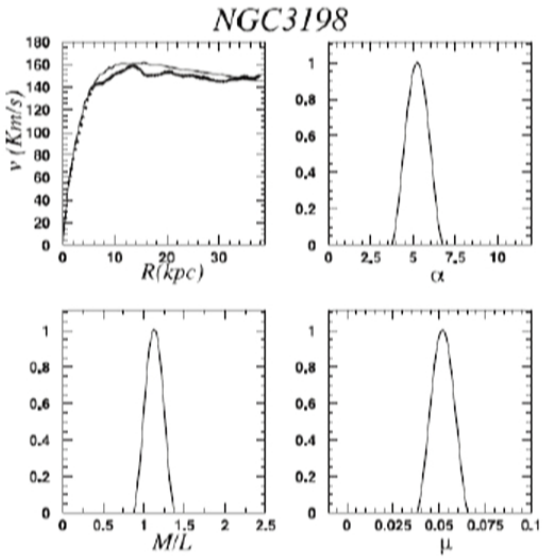
NGC3198
v (Km/s)
R(kpc)
α
M/L
μ

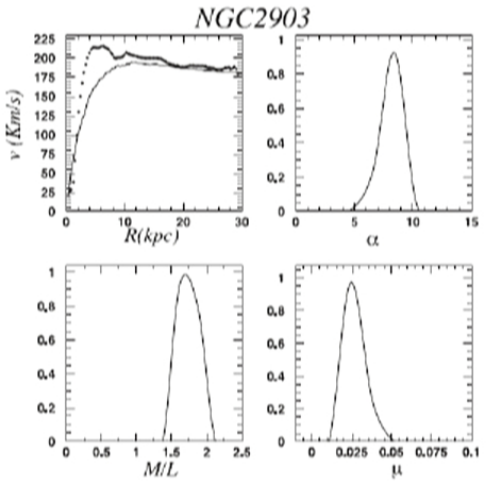
NGC2903
v (Km/s)
R(kpc)
α
M/L
μ

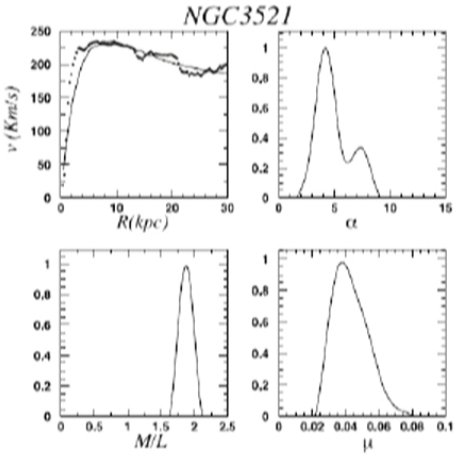
NGC3521
v (Km/s)
R(kpc)
α
M/L
μ

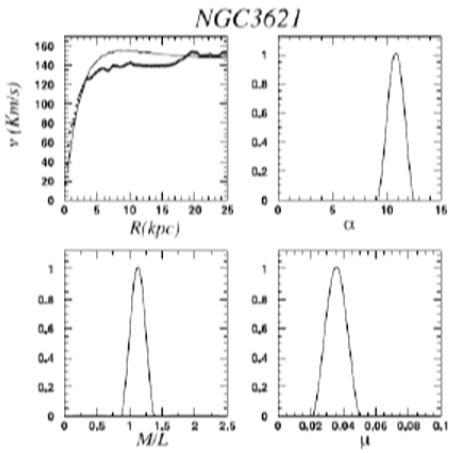
NGC3621
v (Km/s)
R(kpc)
α
M/L
μ

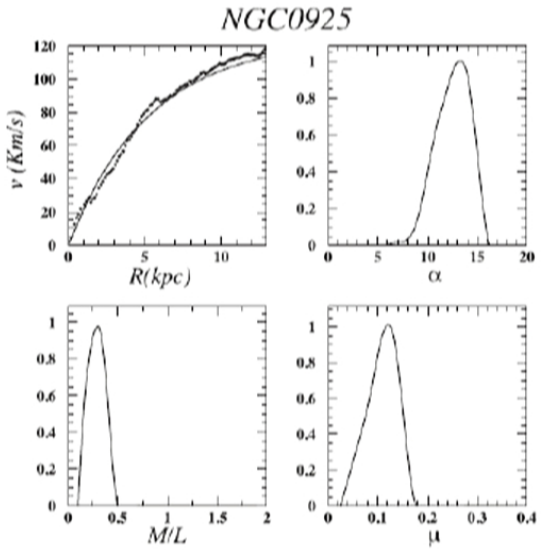

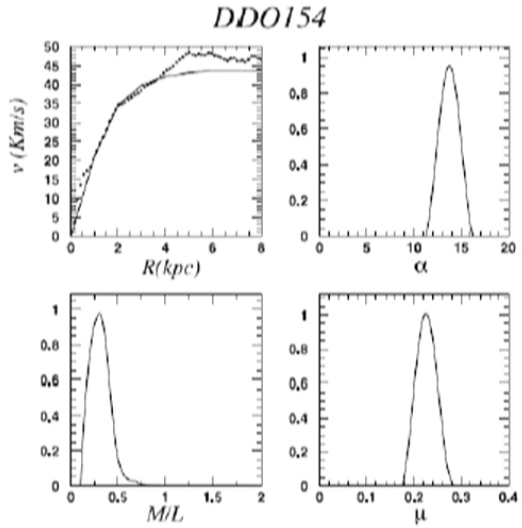

The best fit for the subsample of THINGS galaxies with the corresponding likelihood functions of α, μ and M/L.

From the combined likelihood functions, we obtain the best-fitting parameters of MOG: $\alpha = 8.89 \pm 0.34$ and $\mu = 0.042 \pm 0.004\ \mathrm{kpc}^{-1}$.

We adopt the best-fitting values of α and μ. and let the stellar-to-mass ratio M/L be the only free parameter and obtain fits to the Ursa Major catalogue of galaxies. The average value of χ^2 for all the galaxies is $\overline{\chi^2} = 1.07$.

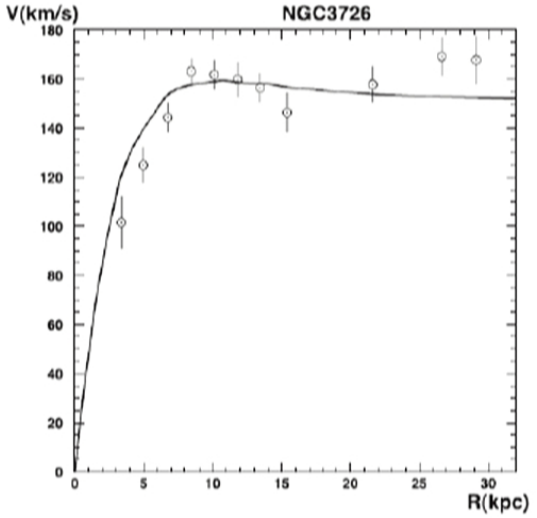

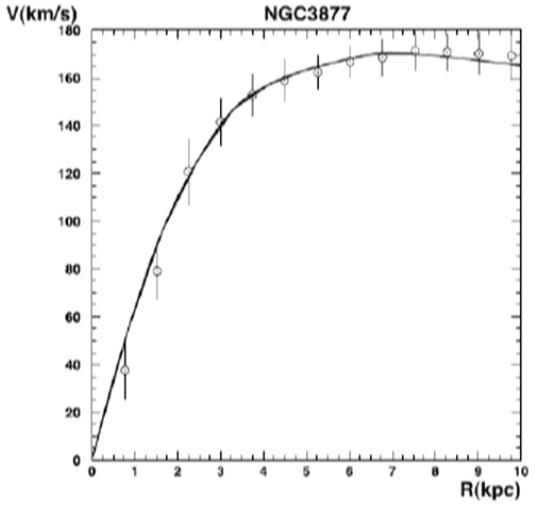

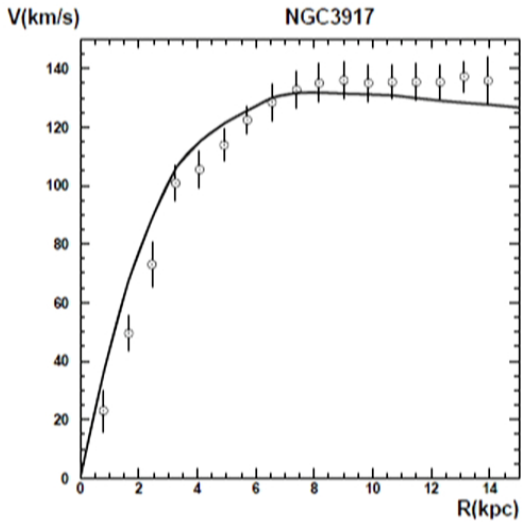
V(km/s)
NGC3917
R(kpc)

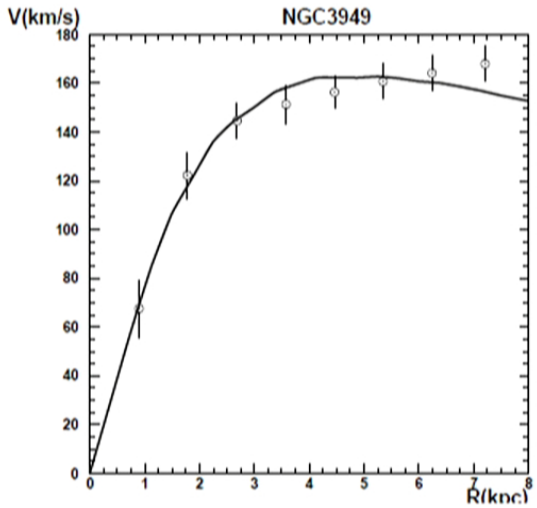
V(km/s)
NGC3949
R(kpc)

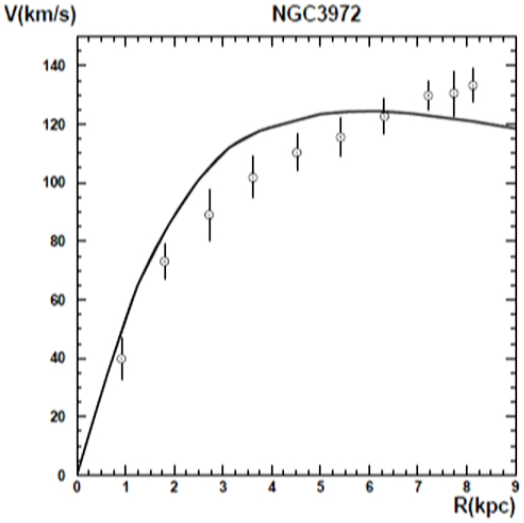
V(km/s)
NGC3972
R(kpc)

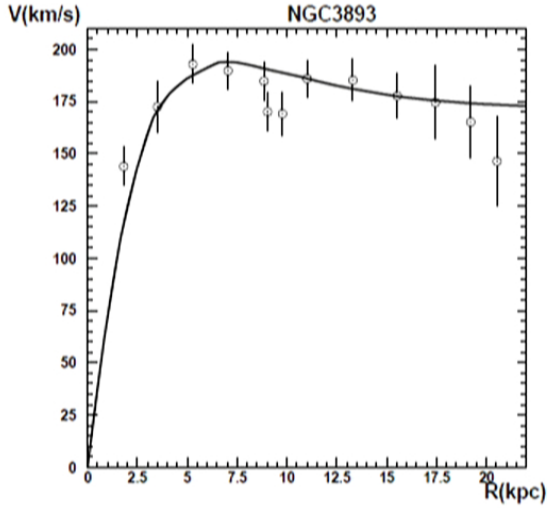
V(km/s)
NGC3893
R(kpc)

Rotation Curve of the Milky Way out to ~ 200 kpc

Pijushpani Bhattacharjee[1,2,3], Soumini Chaudhury[2,4], and Susmita Kundu[2,5]

arXiv:1310.2659 Ap. J. 785, 63 (2014).

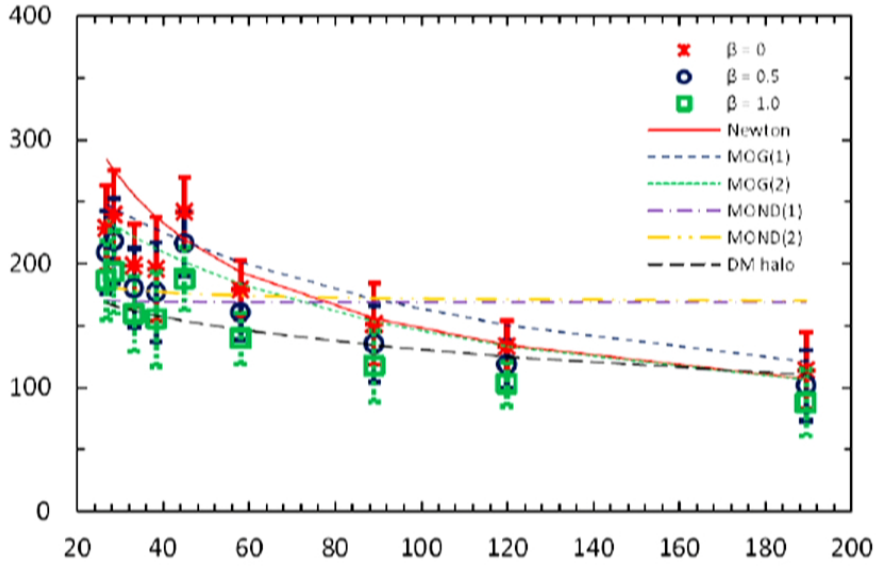

The solid red line is the Newtonian fit with a mass $M = 5 \times 10^{11} M_\odot$. The blue medium dashed and green short dashed lines correspond to MOG using the values $M = 4 \times 10^{10} M_\odot$, $\alpha = 15.01$, $\mu = 0.0313$ kpc^{-1}, and $M = 5 \times 10^{10} M_\odot$, $\alpha = 8.89$, $\mu = 0.04$ kpc^{-1}, respectively. The purple dash-dotted line is MOND with $M = 5 \times 10^{10} M_\odot$, $a_0 = 1.21 \times 10^{-8}$ cm/s^2 The black long - dashed line is the dark matter halo prediction.

We can calculate from the fits to the data the stellar mass-to-light ratio. Also we know the colour of galaxies. On the other hand, the models of stellar evolution predict the dependence of the mass-to-light ratio Υ_* on the colour.

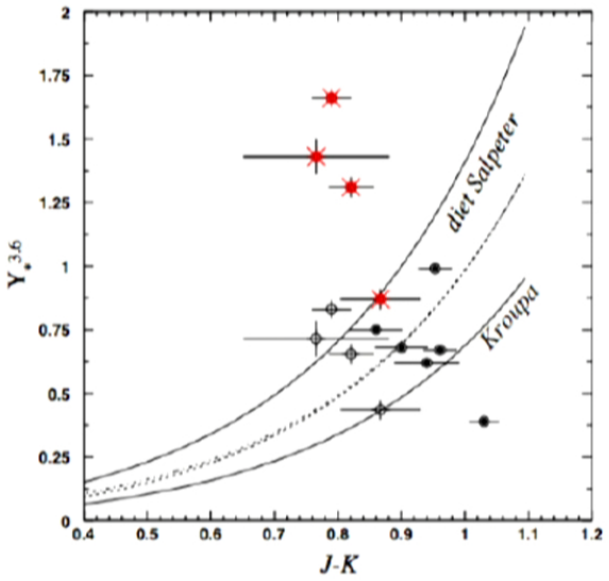

5. Globular Clusters (JWM and V. T. Toth, ApJ. 680, 1158 (2008)).

Fitting velocity dispersions obtained from the Jeans equation to globular cluster data.

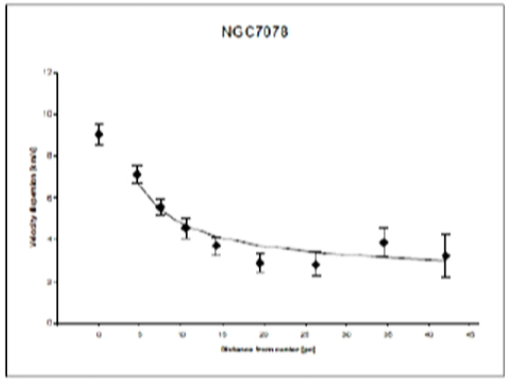

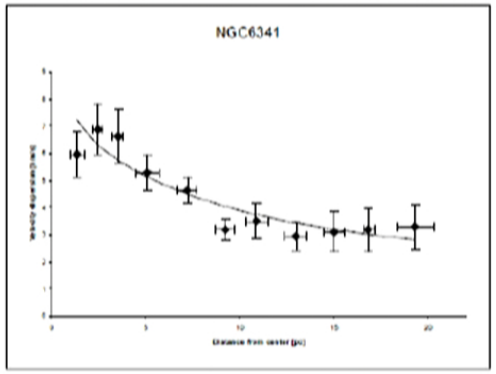

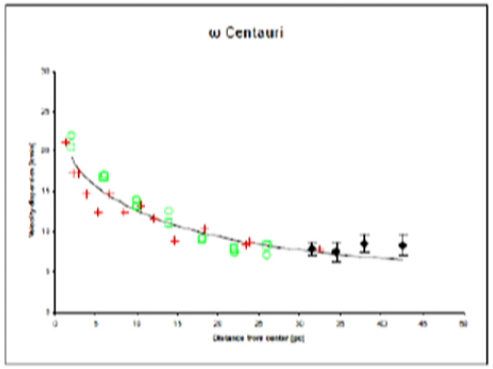

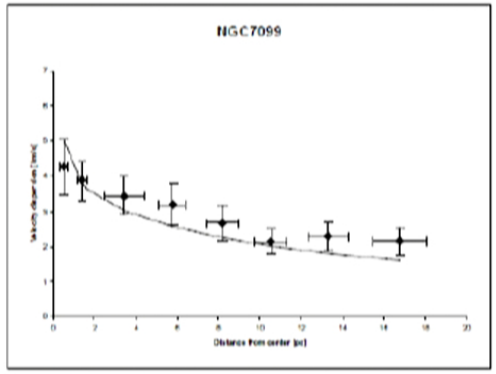

6. CLUSTER DYNAMICS (JWM & S. Rahvar, MNRAS, 441, 3724 (2014), arXiv:1309.5077 [astro-ph]).

We have used the observations of the nearby cluster of galaxies obtained by the Chandra telescope to examine MOG.

Using the Virial theorem or a relaxed spherically symmetric cluster, we can relate the temperature and gas profile to the internal acceleration of the cluster

$$\frac{k_B T(r)}{\mu_p m_p r}\left(\frac{d\ln\rho_g(r)}{d\ln r}+\frac{d\ln T(r)}{d\ln r}\right)=g(r)$$

The left-hand side of this equation is given by data, which has to be consistent with the dynamical mass obtained from the above equation:

$$M_{\rm dyn}(r)=-3.68\times10^{10}\frac{rT(r)}{1+\alpha}\left(\frac{d\ln\rho_g(r)}{d\ln r}+\frac{d\ln T(r)}{d\ln r}\right)$$

We write the overall mass in Newtonian gravity in terms of the MOG dynamical mass:

$$M_{\rm dyn} = \frac{M_N}{1+\alpha}$$

Here, α is already fixed by the fits to the galaxy rotation curves α = 8.89.

The majority of the baryonic cluster mass is gas. For MOG to be consistent with the data, the MOG dynamical mass has to be identically equal to the Newtonian baryonic mass.

We find for the best fit χ^2 value $\beta = M_{\rm dyn}/\breve{M}_{\rm b} = 0.98.$

This yields with a $1\,\sigma$ level of confidence the best value $\beta = 0.98^{+0.02}_{-0.02}$.

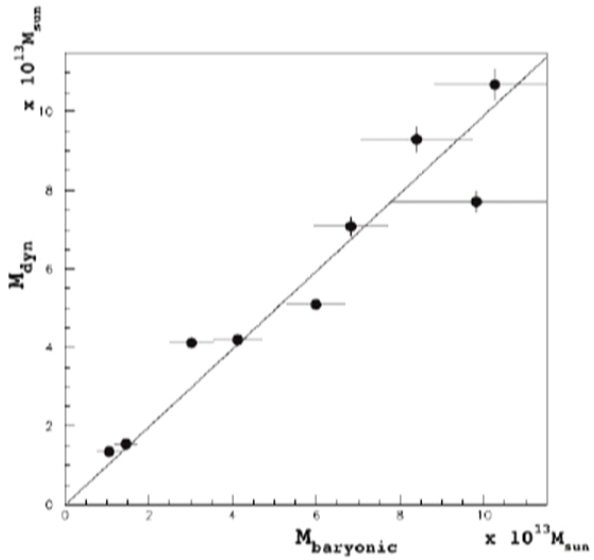

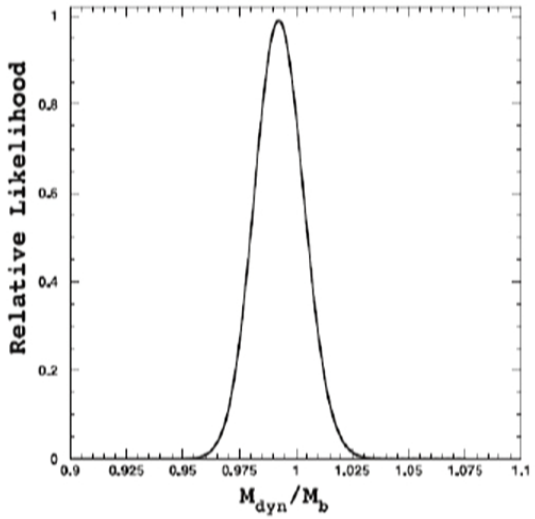

Comparison of the dynamical mass in MOG versus the baryonic mass for clusters. The baryonic mass is composed of gas and stars. The filled circles indicate the corresponding masses up to r_{500} with the corresponding error bars. The solid line shows the best fit to the linear relation $M_{\rm dyn} = \beta_{\rm cl} M_{\rm bar}$ between the two masses with the best fit value of $\beta = 0.99$. The likelihood function for this fit is given in the right-hand panel.

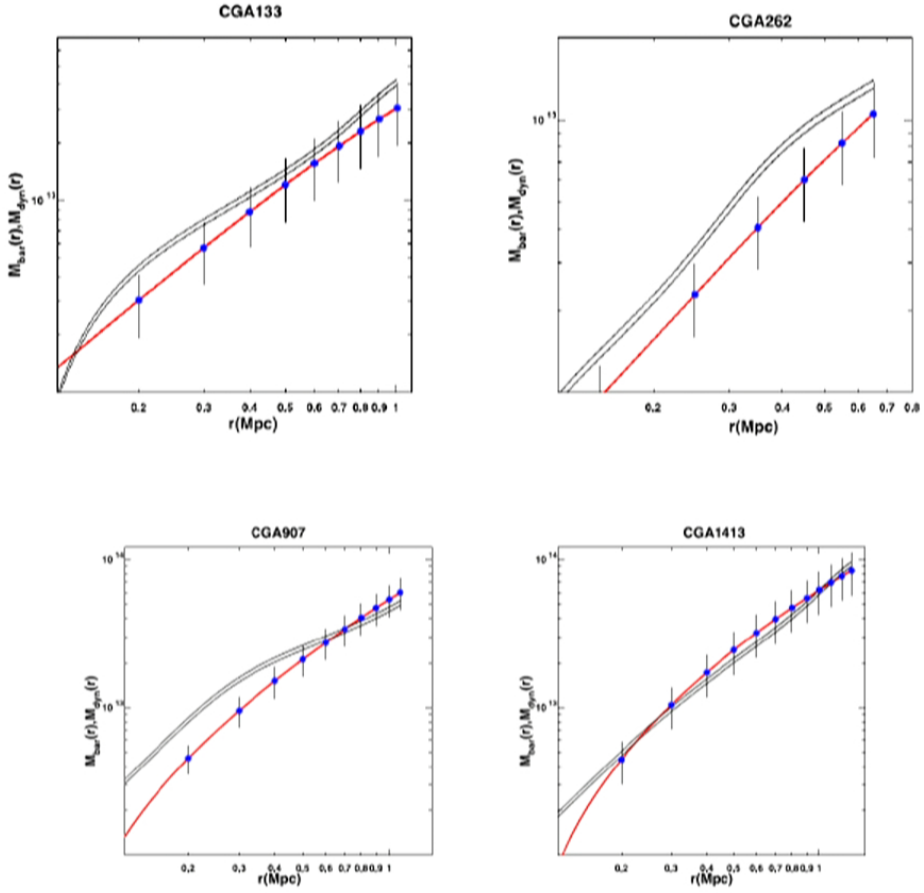
CGA133
CGA262
CGA907
CGA1413
r(Mpc)

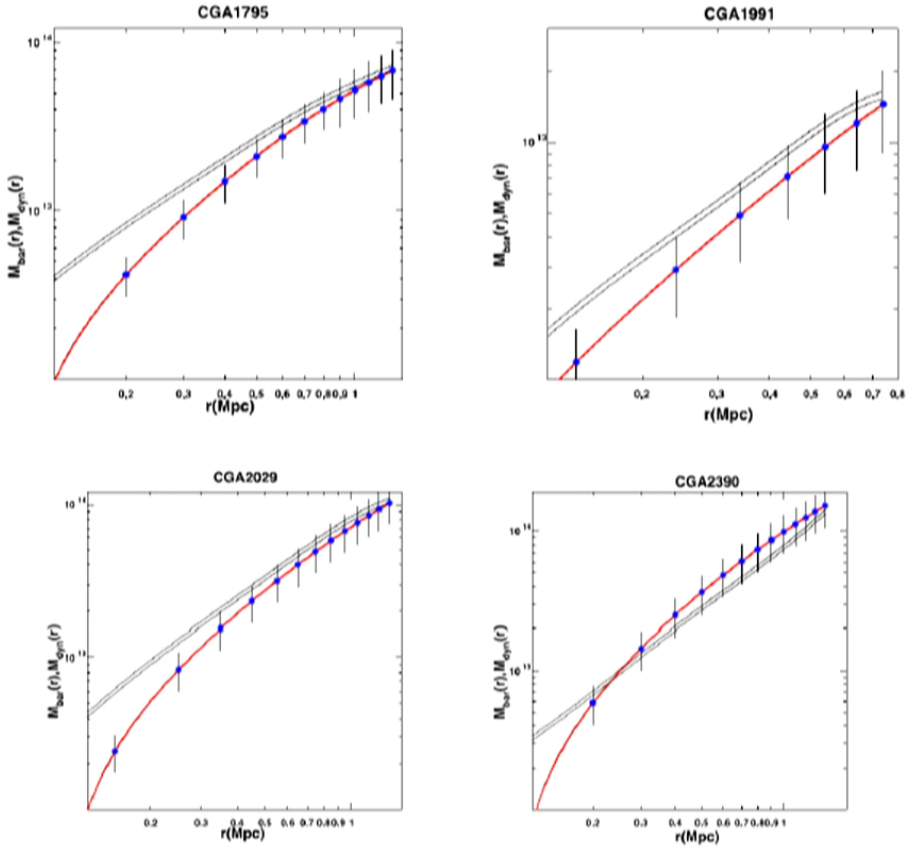

The black solid lines represent the dynamical mass in MOG with the uncertainty resulting from the error bars in the value $\alpha = 8.89 \pm 0.34$. The red line represents the baryonic mass including the masses of the gas and stars in the cluster. The error bars represent uncertainty in the measurements of the cluster mass (Vikhlinin et al. 2006).

7. Bullet Cluster 1E0657-558 and Abell 520 cluster collisions (J. R. Brownstein and JWM, MNRAS, 382, 29 (2007), arXiv:0702146 [astro-ph]).

The κ –convergence predicted by MOG that accounts for the weak and strong lensing by the merging clusters accounts for the off-set of mass observed by Clowe et al. 2006. The relationship between κ and the surface density Σ is given by

$$\kappa(x,y) = \int \frac{4\pi G(r)}{c^2}\frac{D_{\rm l}D_{\rm ls}}{D_{\rm s}}\rho(x,y,z)dz \equiv \frac{\bar{\Sigma}(x,y)}{\Sigma_c},$$

where

$$\bar{\Sigma}(x,y) = \int \mathcal{G}(r)\rho(x,y,z)dz,$$

$$\mathcal{G}(r) \equiv \frac{G(r)}{G_N} = 1+\sqrt{\frac{M_0}{M(r)}}\left\{1-\exp\left(-\frac{r}{r_0}\right)\left(1+\frac{r}{r_0}\right)\right\}$$

$\alpha = \sqrt{\frac{M_0}{M(r)}}$ $\qquad \mathcal{G}_\infty = 1+\sqrt{\frac{M_0}{M}} = 1+\alpha$

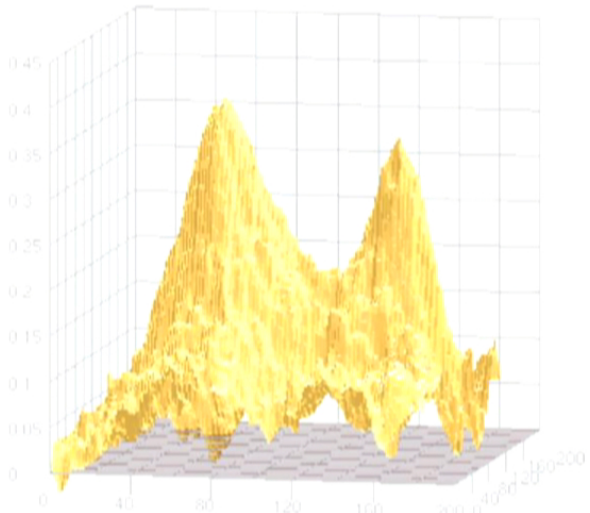

Convergence κ – map data
for Bullet Cluster (Clowe et al 2006).

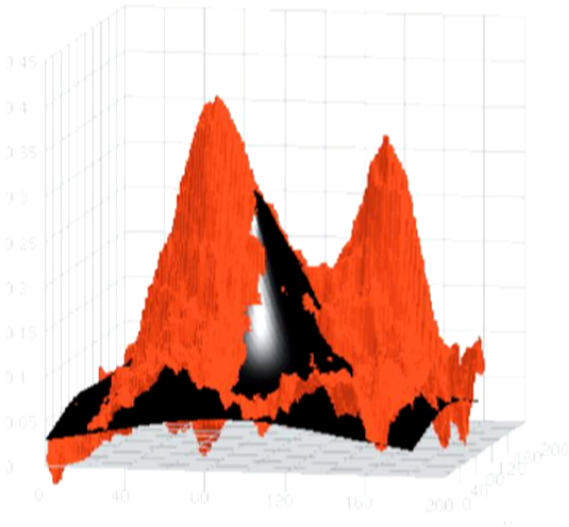

MOG prediction for κ – map convergence.

The fit to the Bullet Cluster data requires no non-baryonic dark matter!

Abell 520 a threat to dark matter models? (Jee et al., ApJ. 747, 96 (2012) arXiv:1202.6368).

Data from NASA's Chandra X-ray Observatory show the hot gas in the colliding clusters colored in green. The gas provides evidence that a collision took place. Optical data from NASA's Hubble Space Telescope and the Canada-France-Hawaii Telescope (CFHT) in Hawaii are shown in red, green, and blue. Starlight from galaxies within the clusters, derived from observations by the CFHT and smoothed to show the location of most of the galaxies, is colored orange.

The blue-colored areas pinpoint the location of most of the mass in the cluster, which is dominated by dark matter. The dark-matter map was derived from the Hubble observations, by detecting how light from distant objects is distorted by the cluster galaxies, an effect called gravitational lensing. The blend of blue and green in the center of the image reveals that a clump of dark matter resides near most of the hot gas, where very few galaxies are found.

This finding confirms previous observations of a dark-matter core in the cluster announced in 2007. The result could present a challenge to basic theories of dark matter, which predict that galaxies should be anchored to dark matter, even during the shock of a powerful collision.

A reconstruction of the Abell 520 data by Clowe et al. (ApJ. 758, 128 (2012), arXiv:1209.2143) do not detect the previously claimed "dark" core at the location of the X-ray plasma. They conclude that A520 shows no evidence to contradict the collisionless dark matter scenario.

MOG can fit the data for Abell 520 , as well as the data for the Bullet Cluster, because the galaxies do not have dark matter haloes and the enhanced lensing is not due to dark matter but to MOG.

8. Conclusions

If experiments continue not to discover dark matter particles in underground experiments, at the LHC and in astrophysical observations, then we should begin to worry that the existence of dark matter can only be inferred from gravity. We must then consider that the law of gravity should be modified. MOG (STVG) can fit all available data from the solar system to galaxies and galactic clusters without detectable dark matter in the present universe.

The hidden massive photon (phion particle) is pressureless and massive enough to act as cold dark matter before decoupling and recombination, allowing for structure growth. The CMB acoustical power spectrum obtained from MOG agrees with the PLANCK 2013 data.

The MOG prediction is that the dark matter phion particle (hidden weakly interacting massive photon) that acts as cold dark matter up till the formation of galaxies, becomes ultra-light in the present universe, $m_\phi = 2.6 \times 10^{-28}$ eV, and undetectable. This can explain the failure to observe dark matter particles today.

A possible generic test that distinguishes the dark matter paradigm in the current universe from MOG can be obtained from future large scale galaxy surveys and the matter power spectrum.

END